Chemical Epigenetics Alters the Secondary Metabolite Composition of Guttate Excreted by an Atlantic-Forest-Soil-Derived *Penicillium citreonigrum*

Xiaoru Wang,[†] José G. Sena Filho,[†,‡] Ashley R. Hoover,[†] Jarrod B. King,[†] Trevor K. Ellis,[†] Douglas R. Powell,[§] and Robert H. Cichewicz*[,†,⊥]

Natural Products Discovery Group, Department of Chemistry and Biochemistry, 620 Parrington Oval, Room 208, and Ecology and Evolutionary Biology Program, University of Oklahoma, Norman, Oklahoma 73019-3032

Received March 4, 2010

Chemical epigenetic manipulation of *Penicillium citreonigrum* led to profound changes in the secondary metabolite profile of its guttate. While guttate from control cultures exhibited a relatively simple assemblage of secondary metabolites, the guttate collected from cultures treated with 50 μM 5-azacytidine (a DNA methyltransferase inhibitor) was highly enriched in compounds representing at least three distinct biosynthetic families. The metabolites obtained from the fungus included six azaphilones (sclerotiorin (**1**), sclerotioramine (**6**), ochrephilone (**2**), dechloroisochromophilone III (**3**), dechloroisochromophilone IV (**4**), and 6-((3*E*,5*E*)-5,7-dimethyl-2-methylenenona-3,5-dienyl)-2,4-dihydroxy-3-methylbenzaldehyde (**5**)), pencolide (**7**), and two new meroterpenes (atlantinones A and B (**9** and **10**, respectively)). While pencolide was detected in the exudates of both control and 5-azacytidine-treated cultures, all of the other natural products were found exclusively in the guttates of the epigenetically modified fungus. All of the metabolites from the *P. citreonigrum* guttate were tested for antimicrobial activity in a disk diffusion assay. Both sclerotiorin and sclerotioramine caused modest inhibition of *Staphylococcus epidermidis* growth; however, only sclerotioramine was active against a panel of *Candida* strains.

Our research group has been actively pursuing the development of chemical epigenetic methods for procuring secondary metabolites from fungi.[1] We have demonstrated that this is an effective technique for promoting the transcription of silent biosynthetic pathways involved in the formation of polyketide, nonribosomal peptide, and hybrid polyketide−nonribosomal-peptide natural products.[2] Moreover, we have shown that a chemical epigenetics approach is well suited for the generation of structurally unique secondary metabolites with promising drug discovery applications.[3,4] In order to maximize the opportunity for detecting novel secondary metabolites, we have begun using chemical epigenetic induction as a routine part of our screening program involving the exploration of fungi obtained from minimally explored environments/ecological niches (e.g., insects and littoral zones[4]).

Our investigation of fungi from ecologically diverse environments has recently expanded to include soil from the Brazilian Atlantic Forest. The Atlantic Forest is regarded as one of the most species-rich habitats in the world, but unfortunately, it is also an exceedingly endangered habitat with <8% of its original 1.3×10^6 km^2 still intact.[5,6] The secondary metabolite profile (observed by HPLC) for one of the solid-state fungal cultures exhibited an exceptionally dramatic response to chemical epigenetic manipulation: in the presence of 5-azacytidine (a DNA methyltransferase inhibitor[1]), the fungus produced rust-red-colored droplets of exudate on its mycelial surface, whereas untreated (control) cultures produced colorless exudates.

Fungal exudates, which are more formally known as guttates, are observed with considerable frequency in solid-state fungal cultures. Despite the widespread occurrence of this phenomenon, a surprisingly small number of accounts have been published exploring the composition of fungal guttates. The few studies that do exist suggest that these droplets are a rich source of primary and secondary metabolites, inorganic substances, and proteins/enzymes.[7−11] For example, strains of *Penicillium nordicum* and *Penicillium verrucosum* grown for 14 days on Petri plates containing Czapek yeast agar were reported to have accumulated substantial amounts of guttate, which was enriched in ochratoxins A and B (on average, approximately 1−8 μg/mL).[11] Similarly, cultures of *Metarhizium anisopliae* that were reared on several different media accumulated destruxins A, B, and E in their exudates at levels averaging 2−6 μg/mL.[7] The ecological significance of guttation remains uncertain, although several possible functions have been proposed. These roles include facilitating active hyphal expansion under conditions of unfavorable water potential,[12] providing a mechanism for transporting enzymes that are involved in host invasion and/or liberation of essential nutrients from substrates,[10,13,14] and creation of unique microhabitats capable of supporting symbiotic bacterial communities.[15−17]

In light of the striking guttate coloration induced in the Atlantic Forest fungal isolate, we initiated this project to discern what changes occurred to the chemical diversity of the fungal guttate upon treatment of the organism with 5-azacytidine. In this report, we demonstrate that chemical epigenetic manipulation led to a substantial restructuring of secondary metabolite pools in the guttate produced by an Atlantic-Forest-derived fungal isolate.

Results and Discussion

The sequence of a 321-base-pair portion of the large ribosomal subunit 28S rRNA gene from the Atlantic-Forest-soil-derived isolate was identical to the sequence reported in the NCBI database for *Penicillium citreonigrum* Dierckx (syn. *Eupenicillium hirayamae* D. B. Scott & Stolk). Growth of the fungus on a vermiculite-based solid-state medium containing 0, 10, 50, 100, or 200 μM 5-azacytidine showed that cultures exposed to ≥50 μM of the epigenetic modifier developed dark red guttates, which stood in vivid contrast to the colorless guttates produced by control cultures (Figure 1, A and B). Gradient HPLC was used to compare the guttates from 20-day-old control cultures versus fungal colonies treated with 50 μM 5-azacytidine. Whereas the control guttates were relatively devoid of small molecules, the HPLC profiles of guttates from

* To whom correspondence should be addressed. Tel: (405) 325-6969. E-mail: rhcichewicz@ou.edu.
[†] Natural Products Discovery Group, Department of Chemistry and Biochemistry.
[‡] Current address: Empresa Brasileira de Pesquisa Agropecuária-EMBRAPA, Coastal Tablelands, Av. Beira Mar, 3250, 49025-040, Aracaju, SE, Brazil.
[§] Department of Chemistry and Biochemistry.
[⊥] Ecology and Evolutionary Biology Program.

10.1021/np100142h
Published on Web 05/07/2010

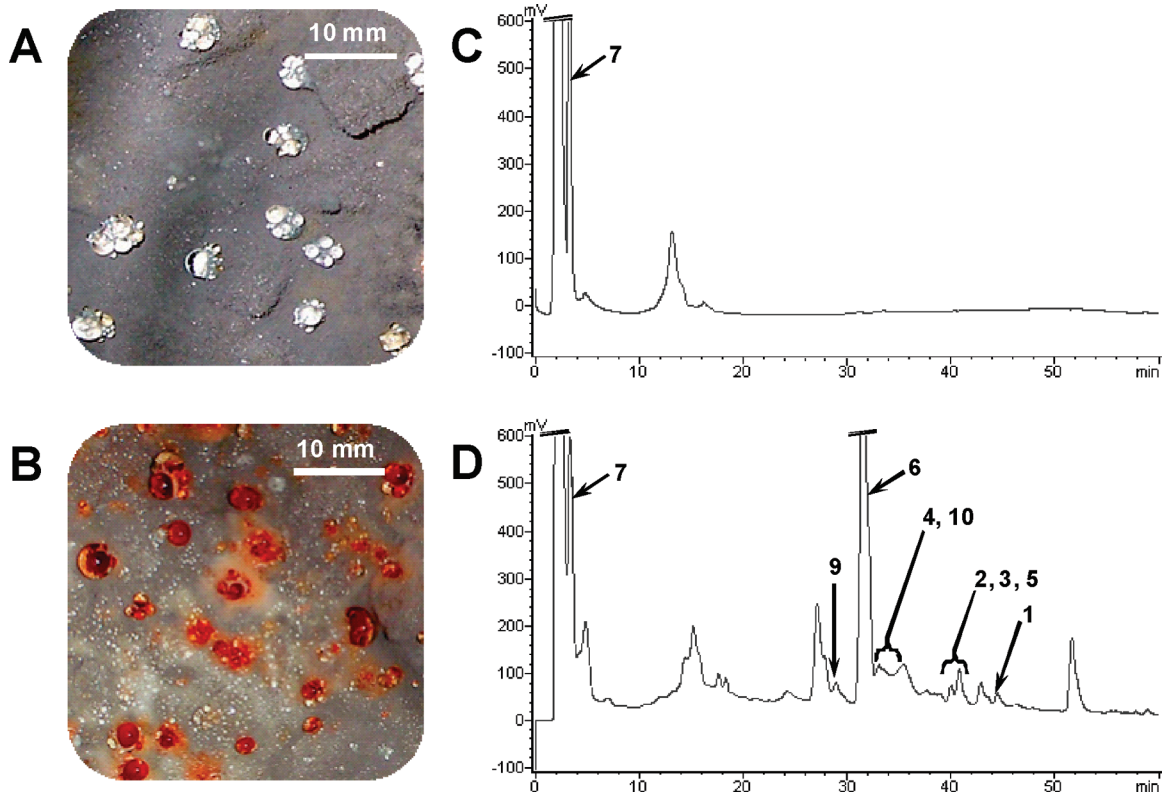

Figure 1. Guttates of solid-state *P. citreonigrum* cultures grown under control conditions (A) or in the presence of 50 μM 5-azacytidine (B). HPLC chromatograms (C_{18} column using a gradient of 30−100% CH_3CN in H_2O and recorded at 210 nm) illustrating the differences between the metabolite profiles of the control (C) and 5-azacytidine-treated (D) *P. citreonigrum* guttates. Metabolites identified in scale-up isolation studies were used as authentic references to verify the identities of compounds **1**−**7**, **9**, and **10** in the guttates.

5-azacytidine-treated cultures were highly enriched in secondary metabolites (Figure 1, C and D).

Scale-up solid-state cultures of *P. citreonigrum* treated with 50 μM 5-azacytidine were prepared, and after 20 days the resulting guttate-covered mycelia were washed with EtOAc. The EtOAc was removed under vacuum, and the remaining solid residue was resuspended in MeOH prior to defatting with hexane. The MeOH-soluble material was subjected to repeated C_{18} gradient HPLC, which yielded six pigmented compounds that ranged in color from yellow-orange to dark red. A combination of ^{1}H and ^{13}C NMR, specific rotation, and HRESIMS data facilitated the rapid dereplication of five azaphilones.[18] These compounds were determined to be sclerotiorin (**1**),[19,20] ochrephilone (**2**),[21] dechloroisochromophilone III (**3**),[22] dechloroisochromophilone IV (8-acetyldechloroisochromophilone III) (**4**),[22] and 6-((3*E*,5*E*)-5,7-dimethyl-2-methylenenona-3,5-dienyl)-2,4-dihydroxy-3-methylbenzaldehyde (**5**).[22]

A sixth, highly colored substance (red solid) was obtained that exhibited ^{1}H and ^{13}C NMR data that were remarkably similar to the chemical shifts observed for **1**−**5**. Interpretation of the HRESIMS and NMR data for **6** revealed that our metabolite matched the structure reported for sclerotioramine (**6**), which had been previously obtained as a semisynthetic derivative of **1**.[23] Unfortunately, we were unable to find any NMR data published for this substance, so we performed a thorough analysis of **6** using $^{2-3}J_{H-C}$ HMBC NMR spectroscopy to facilitate the assignment of its proton and carbon resonances. An important step in our investigation was confirming the location of the amine nitrogen in ring B. This was achieved by comparing the upfield changes in the chemical shifts for the C-1 and C-3 resonances (δ_C 138.4 and 146.1, respectively) in **6** to the corresponding C-1 and C-3 chemical shifts surrounding the oxygen atom in compound **1** (δ_C 152.6 and 158.1, respectively).

Although **6** had not been previously described as a natural product, other nitrogen-containing azaphilones have been reported from fungal sources.[24,25] These vinylogous γ-pyridone metabolites are thought to arise from the substitution of a primary amine/ammonia for the azaphilone's pyranyl oxygen atom in a process that is initiated by the nucleophilic attack of the nitrogen at the C-1 position.[24] Therefore, we can reasonably surmise that **6** is formed as a consequence of **1** reacting with endogenous ammonia from *P. citreonigrum* during the culture process.[26]

Compound **7** was obtained as a colorless solid that exhibited a *m/z* of 218.0432 $[M + Na]^+$ by HRESIMS. This established a molecular formula of $C_9H_9NO_4$ for **7**, which required six units of unsaturation. Analysis of the NMR data for the metabolite (^{1}H, ^{13}C, $^1J_{H-C}$ HSQC, and $^{2-3}J_{H-C}$ HMBC) led us to determine that the structure of **7** was the same as the structure that had been previously proposed for pencolide.[27] Although this metabolite had been encountered on at least two prior occasions from *Penicillium* species,[27−29] no detailed investigation concerning both its ^{1}H and ^{13}C NMR resonances had been reported. Moreover, debate that had arisen concerning the C-2, C-3 double-bond configuration of **7** had not yet been fully resolved.[30−32] Therefore, we investigated the double-bond configuration of **7** by treating it with thionyl chloride in MeOH, which yielded the methyl ester derivative **8**. Using one-dimensional nuclear Overhauser effect difference correlation (1D difference NOE) spectroscopy, we observe reciprocal NOEs between the olefinic H-3 proton (δ_H 7.30) and the protons of the C-1 methyl ester (δ_H 3.73). In contrast, irradiation of the C-4 methyl protons (δ_H 1.77) provided enhancement only of the H-3 resonance. These findings strongly support a *Z* configuration for the C-2, C-3 double bond in **7**.

HRESIMS analysis of compound **9** provided a pseudomolecular ion with a *m/z* of 465.2256 $[M + Na]^+$, which was consistent with a molecular formula of $C_{26}H_{34}O_6$. This required 10 degrees of unsaturation in the metabolite. A survey of the ^{13}C NMR data for **9** collected in $CDCl_3$ (Table 1) confirmed the presence of 26 unique carbon atoms including two ketone (δ_C 209.6 and 211.3), two ester

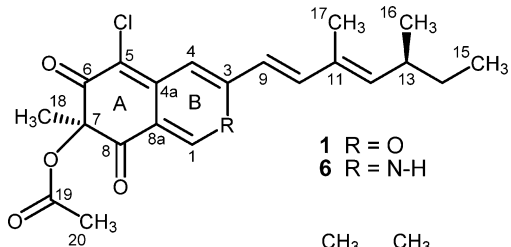

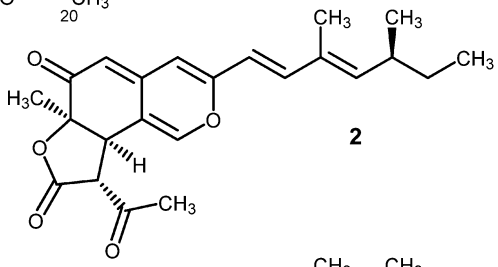

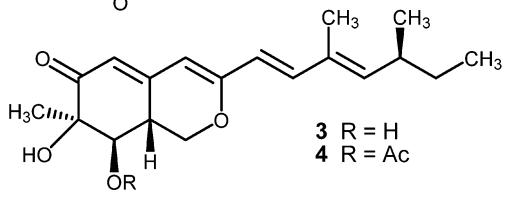

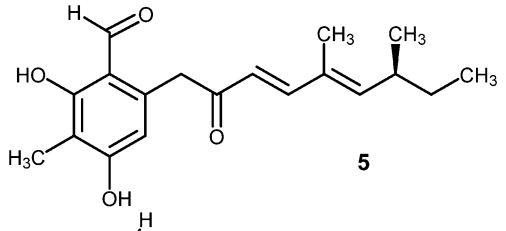

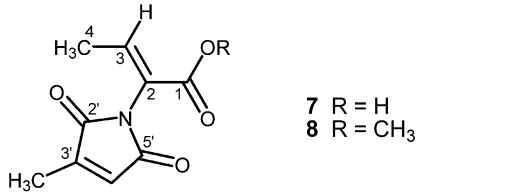

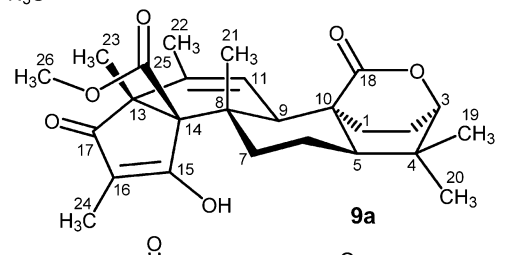

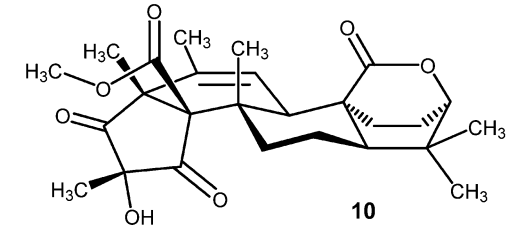

(δ_C 168.3 and 174.8), and two vinylic carbon (δ_C 127.4 and 132.0) resonances. This accounted for five of the 10 double-bond equivalents in **9**, which meant that the remaining units of unsaturation were derived from five rings. Examination of the ^{1}H NMR data (Table 1) revealed six methyl singlets (δ_H 1.02, 1.07, 1.32 (×2), 1.69, and 3.54; each integrated for 3H), a methyl doublet (δ_H 1.19, J = 6.8 Hz, 3H), a vinylic hydrogen singlet (δ_H 5.67, 1H), a doublet (δ_H 4.07, J = 3.6 Hz, 1H), a quartet (δ_H 3.20, J = 6.8 Hz, 1H), and a series of overlapping multiplets spanning the region δ_H 1.0−2.4. The congestion caused by multiple resonances overlapping in the upfield region of the ^{1}H NMR spectrum prompted us to explore other solvents for performing NMR experiments with **9**. Turning to CD_3OD, we were surprised by two significant qualitative changes in the ^{1}H NMR spectrum (Table 1): the methyl doublet previously at δ_H 1.19 now appeared as a singlet (δ_H 1.57, 3H) and the quartet at δ_H 3.20 was missing. Upon reexamination of the $^1J_{H-C}$ HSQC data for **9** collected in $CDCl_3$, we observed that the missing hydrogen had been bonded to a carbon resonating at δ_C 51.4. The ^{13}C NMR data for **9** collected in CD_3OD (Table 1) exhibited other substantial changes that included both the loss of a ketone resonance (δ_C 211.3) and the carbon at δ_C 51.4. In place of the missing carbon spins, we observed two new vinylic carbon resonances appearing at δ_C 113.7 and 192.1. The substantial downfield shift of the vinylic carbon at δ_C 192.1 suggested that it was attached to an oxygen atom. The $^{2-3}J_{H-C}$ HMBC data for **9** in CD_3OD revealed that the protons of the methyl singlet at δ_H 1.57 not only coupled with both of the vinylic carbons but also exhibited a correlation to a ketone resonance at δ_C 201.8 (Figure 2A, fragment A). This led us to deduce that compound **9** possessed a tautomerizable substructure that existed in its keto−enol form in CD_3OD (**9a**) and rearranged into a β-diketone in $CDCl_3$ (**9b**) (Figure 3). We confirmed this by removing **9** from the CD_3OD and resuspending the compound in $CDCl_3$. This provided ^{1}H and ^{13}C NMR and HRESIMS data for the metabolite that were identical to those we had previously observed for **9b**.

Having established the tautomeric portion of the new metabolite (Figure 2A, fragment A), we focused our attention on determining the remaining structural elements of **9a/9b**. We noted that the ^{1}H and ^{13}C NMR resonances associated with the rest of the metabolite in **9a** and **9b** appeared very similar to one another (Table 1). Therefore, we concentrated on using the 2D NMR data set collected for **9a** as the basis for resolving the rest of this compound's structure. Examination of the $^{2-3}J_{H-C}$ HMBC data for **9a** enabled us to construct four additional substructures for the metabolite (Figure 2A, fragments B−E).

The development of fragment B (Figure 2A) was largely facilitated by the fortuitous proximity of three methyl groups and one olefinic proton, which provided a nearly exhaustive set of overlapping $^{2-3}J_{H-C}$ HMBC correlations among the substructure's nine carbon atoms. The first methyl singlet (δ_H 1.36) exhibited a series of three couplings with carbon resonances at δ_C 43.0, 47.6, and 69.8. The second methyl singlet (δ_H 1.22) was also correlated to the carbon at δ_C 69.8, as well as carbons at δ_C 57.5 and 134.7. The third methyl singlet (δ_H 1.82) shared two of the same correlations (δ_C 57.5 and 134.7), as well as an additional coupling to a carbon at δ_C 126.3. Finally, the olefinic singlet proton (δ_H 5.44) was coupled to a methyl carbon (δ_C 20.3) and carbons at δ_C 43.0 and 57.5. The combination of these overlapping $^{2-3}J_{H-C}$ couplings enabled us to deduce that fragment B constituted a highly substituted cyclohexene system (Figure 2A, fragment B).

Initially, the array of $^{2-3}J_{H-C}$ couplings in CD_3OD for fragment C appeared perplexing and structurally uninformative; however, by expanding our assessment of this portion of **9** to include additional HMBC couplings detected in $CDCl_3$, we were able to derive three sets of ^{1}H → ^{13}C correlations that were useful for revealing the composition of this substructure. The first set consisted of correlations from a doublet proton at δ_H 4.07 (J = 3.6 Hz, 1H) to carbons at δ_C 22.6, 32.6, 51.3, and 174.8. Upon considering the chemical shifts of these carbons and their respective numbers of attached protons (determined by $^1J_{H-C}$ HSQC), we were able to deduce that they represented two aliphatic methyl groups, a methylene, and a quaternary carbon, respectively. We also noted a strong ^{1}H−^{1}H COSY correlation from the proton at δ_H 4.07 to geminal protons attached to the carbon at δ_C 21.8 [based on $^1J_{H-C}$ HSQC; δ_H 1.89 (m, 1H) and 2.07 (m, 1H)]. These protons in turn coupled with a second set of geminal protons (δ_H 1.39, m, 1H, and δ_H 2.05, m, 1H) that were attached to a carbon at δ_C 32.6 (based on $^1J_{H-C}$ HSQC). Additional $^{2-3}J_{H-C}$ couplings were found that originated from a methyl singlet at δ_H 1.02 and extended out to carbons at δ_C 28.1, 37.4, 51.3, and 84.4, as well as from a proton

Table 1. ^{1}H (500 MHz) and ^{13}C (125 MHz) NMR Data for **9a** (CD_3OD), **9b** ($CDCl_3$), and **10** ($CDCl_3$)

	atlantinone A (**9a**)			atlantinone A (**9b**)			atlantinone B (**10**)		
position	δ_C, mult.	δ_H (J in Hz)	HMBC[a]	δ_C, mult.	δ_H (J in Hz)	HMBC[a]	δ_C, mult.	δ_H (J in Hz)	HMBC[a]
1	33.5, CH_2	1.48, m	3, 5, 10	32.6, CH_2	1.39, m	18	32.6, CH_2	1.43, m	3, 10
		2.04, dd (3.0, 13.5)	6		2.05, m			2.09, m	
2	22.9, CH_2	2.17, dt (3.0, 13.5)	5, 18	21.8, CH_2	2.07, m	5	21.8, CH_2	2.13, m	1
		1.88, m	3		1.89, m	3		1.95, m	3
3	86.1, CH	4.12, d (3.7)	2, 5, 18	84.4, CH	4.07, d (3.6)	1, 5, 18, 19	84.4, CH	4.11, d (4.0)	1, 2, 5, 18
4	38.4, C			37.4, C			37.4, C		
5	52.9, CH	1.50, t (3.7)	6, 18, 20	51.3, CH	1.44, m	2, 4, 6, 20	51.2, CH	1.49, m	1, 4, 18
6	23.2, CH_2	1.60, m	5	21.9, CH_2	1.56, m	8, 10	21.8, CH_2	1.50, d (13.0)	
		1.37, m	5		1.42, m	5, 10		1.60, m	
7	32.9, CH_2	2.10, dt (3.1, 13.5)	5, 9	30.1, CH_2	2.39, m	8	30.0, CH_2	2.58, td (4.5, 13.0)	5, 8, 9
		2.08, dd (3.0, 13.5)	5, 9		2.28, dt (13.7, 3.5)	5		2.25, m	14
8	43.0, C			39.7, C			38.8, C		
9	47.6, CH	1.90, m	18, 21	47.2, CH	1.82, m	11, 12	46.6, CH	1.96, t (3.0)	8, 11, 18
10	46.7, C			45.0, C			45.0, C		
11	126.3, CH	5.44, s	8, 10, 13, 22	127.4, CH	5.67, s	9, 10, 13, 22	129.4, CH	5.82, s	8, 9, 13, 22
12	134.7, C			132.0, C			131.0, C		
13	57.5, C			61.1, C			61.3, C		
14	69.8, C			73.3, C			71.7, C		
15	192.1, C			211.3, C			211.5, C		
16	113.7, C			51.4, CH	3.20, q (6.8)	15, 17, 24	72.5, C		
17	201.8, C			209.6, C			207.5, C		
18	178.1, C			174.8, C			174.9, C		
19	22.8, CH_3	1.03, s	4, 20	22.6, CH_3	1.02, s	3, 4, 5, 20	22.6, CH_3	1.06, s	3, 4, 5, 20
20	28.3, CH_3	1.14, s	4, 19	28.1, CH_3	1.07, s	3, 4, 5, 19	28.0, CH_3	1.12, s	3, 4, 5, 19
21	17.6, CH_3	1.36, s	7, 8, 9, 14	16.5, CH_3	1.32, s	7, 8, 10	16.9, CH_3	1.35, s	7, 8, 9, 14
22	20.3, CH_3	1.82, s	11, 12, 13	19.2, CH_3	1.69, s	11, 12, 13, 14	19.1, CH_3	1.76, s	11, 13
23	16.7, CH_3	1.22, s	12, 13, 14, 17	16.5, CH_3	1.32, s	12, 13, 14, 17	17.7, CH_3	1.41, s	12, 13, 14, 17
24	6.7, CH_3	1.57, s	15, 16, 17	9.6, CH_3	1.19, d (6.8)	15, 16, 17	19.9, CH_3	1.38, s	15, 16, 17
25	172.7, C			168.3, C			167.6, C		
26	52.0, CH_3	3.58, s	25	52.0, CH_3	3.54, s	25	52.1, CH_3	3.61, s	25
OH								2.22, brs	15, 16, 17, 24

[a] HMBC correlations, optimized for 8 Hz, are from the proton(s) stated to the indicated carbon(s).

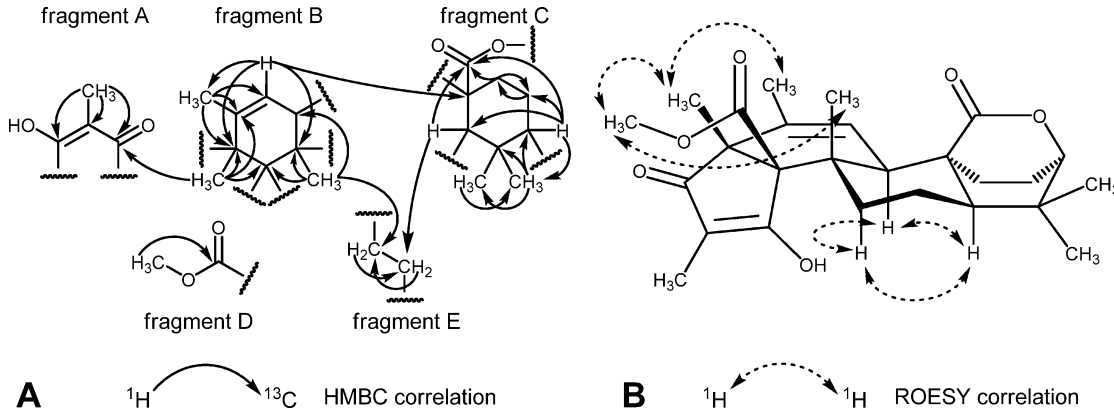

Figure 2. Selected correlations obtained from a $^{2-3}J_{H-C}$ HMBC experiment that were used to generate fragments A−F, which were critical for deducing the structure of **9a** (A). Key ^{1}H−^{1}H ROESY correlations that were used to help assign the relative configuration of **9a** (B).

at δ_H 1.44 to carbon resonances at δ_C 21.8, 28.1, 37.4, and 174.8. The abundance of carbons shared among at least two of the three sets of $^{2-3}J_{H-C}$ couplings enabled us to construct a cyclohexane substructure with an ester and geminal methyl groups at the 1- and 3-positions, respectively (Figure 2A, fragment C). Further consideration of the downfield shift observed for the carbon at δ_C 84.4 and the $^3J_{H-C}$ coupling exhibited by its attached proton to the ester carbonyl resonance (δ_C 174.8) led us to deduce the presence of a second fused ring in fragment C. Thus, fragment C was proposed to consist of a 6,6-dimethyl-2-oxabicyclo[2.2.2]octan-3-one system (Figure 2A).

With the establishment of fragments A−C, only a handful of atoms remained to be assigned ($C_4H_7O_2$). Three of the remaining protons belonged to a methyl singlet (δ_H 3.58, 3H) that was judged by its chemical shift and $^3J_{H-C}$ HMBC coupling to be associated with an ester carbonyl (δ_C 172.7). Given that no other correlations were observed from the other fragments to any of the atoms in fragment D (Figure 2A), we waited to assign its position in the metabolite until other evidence was secured. Fragment E (Figure 2A) was determined to be composed of two methylenes on the basis of ^{1}H−^{1}H COSY data showing the coupling of their attached protons (geminal protons at δ_H 1.60 and 1.37 coupled to a second set of geminal protons at δ_H 2.10 and 2.08).

With all of the atoms accounted for in **9**, the final task was to determine the linkages among fragments A−E. Reexamination of the $^{2-3}J_{H-C}$ HMBC data showed that the methyl protons at δ_H 1.22 in fragment B exhibited a $^3J_{H-C}$ coupling with the ketone resonance (δ_C 201.8) in fragment A. With no other $^{2-3}J_{H-C}$ couplings apparent, we considered the fact that one of the quaternary carbons in fragment B (δ_C 69.8) was still lacking two of its four required bonding groups. We deduced that the enol carbon (δ_C 192.1) in fragment A was joined to this quaternary carbon in fragment B,

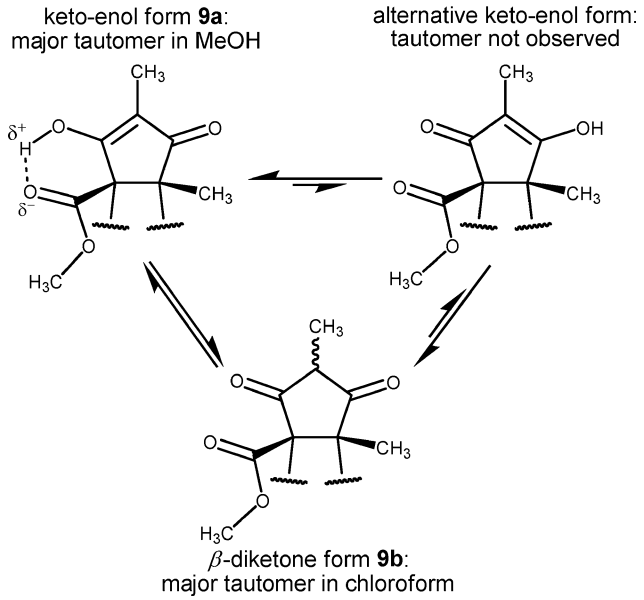

Figure 3. Possible tautomers proposed for compound **9**. The enol−keto structure **9a** (upper left) was the only tautomer observed in MeOH, while the β-diketone compound **9b** (lower center) was exclusively seen in chloroform. The alternative enol−keto form of **9** (upper right) was not detected by NMR under these experimental conditions.

which resulted in a five-membered 3-hydroxy-2-methylcyclopent-2-enone system. A series of three additional $^{2-3}J_{H-C}$ HMBC couplings were detected that allowed us to link fragments B, C, and E (fragment B δ_H 1.36 → fragment E δ_C 32.9, fragment B δ_H 5.44 → fragment C δ_C 46.7, and fragment C δ_H 1.50 → fragment E δ_C 23.2), and this enabled us to establish the final ring system required for **9**. With only two unbonded carbon atoms left, we concluded that the ester comprising fragment D must be attached to the remaining quaternary carbon (δ_C 69.8) in fragment B.

With the planar structure of **9a** established, the assignment of the relative configuration for each of the compound's asymmetric centers was addressed by a 2D ^{1}H−^{1}H ROESY experiment. We observed a set of reciprocal correlations among several of the cyclohexene's substituents including H-22 ↔ H-11 and H-23, H-23 ↔ H-26 and H-21, and H-26 ↔ H-21 (Figure 2B). These data supported a *cis* fusion between the five-membered 3-hydroxy-2-methylcyclopent-2-enone and the cyclohexene ring systems. In addition, we detected reciprocal ^{1}H−^{1}H ROESY correlations among three of the four axial protons of the cycloalkane (H-7$_{axial}$ ↔ H-9$_{axial}$ ↔ H-5$_{axial}$) (Figure 2B). This enabled us to establish the relative configuration of **9a** as 3*R**,5*R**,8*S**,9*R**,10*S**,13*R**,14*R**. During the process of characterizing the structure of **9a**, we were able to secure a crystal of the metabolite from MeOH that was suitable for X-ray crystallography. An ORTEP drawing of **9a** derived from the X-ray diffraction analysis is illustrated in Figure 4. In addition to verifying the proposed relative atom configuration for **9a**, we were also able to confirm the compound's absolute configuration as 3*R*,5*R*,8*S*,9*R*,10*S*,13*R*,14*R*. Considering the unique Atlantic Forest habitat from which the *P. citreonigrum* strain was obtained, we have given **9** the name atlantinone A.

At this point in the investigation, we returned our attention to the occurrence and population distribution of the three potential tautomers of **9** (Figure 3). Whereas the keto−enol tautomer **9a** (Figure 3) was readily apparent in MeOH (C-17 ketone and C-15 enol carbon), we were not able to detect any traces of the complementary keto−enol tautomer (C-15 ketone and C-17 enol carbon) in solution. We suspect this may be due to the stabilizing influence of intramolecular hydrogen bonding between the C-15 enol hydroxy group and the C-25 carbonyl oxygen atom. However,

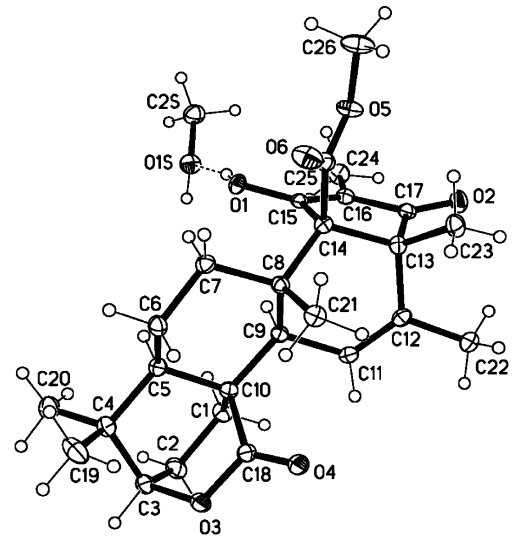

Figure 4. ORTEP structure generated from the X-ray diffraction data for a single crystal of **9a** that was obtained from MeOH.

it is interesting to note that neither the andrastins[33] nor citreohybridonol,[34] which share similar *cis*-fused cyclohexene and 3-hydroxy-2-methylcyclopent-2-enone substructures with **9**, is reported to exhibit a preference in MeOH or chloroform for a single tautomeric species. Instead both sets of compounds undergo rapid transitions between their keto−enol and β-diketone forms in solution. We also noted that the corresponding β-diketone **9b** was the only form of the metabolite observed in chloroform. Examination of ^{1}H−^{1}H ROESY data for **9b** in $CDCl_3$ showed that both 16*R* and 16*S* configurations were present in solution (correlations between H-24 ↔ H-9 and H-24 ↔ H-26 were observed).

A related metabolite (**10**) was detected in one of the HPLC fractions that eluted just after **9**. HRESIMS showed that **10** varied from the latter by the addition of an oxygen atom (*m*/*z* 481.2203 $[M + Na]^+$ consistent with a molecular formula of $C_{26}H_{34}O_7$). The ^{1}H and ^{13}C NMR data for **10** collected in $CDCl_3$ (Table 1) showed remarkable similarity to **9b** with one exception: C-16 was shifted substantially downfield (δ_C 72.5 in **10** versus δ_C 51.4 in **9b**) and its attached proton was missing (based on $^1J_{H-C}$ HSQC). This suggested that **10** was the C-16 hydroxy analogue of **9b**, and it was given the name atlantinone B. The remaining structural similarity between **10** and **9b** was quickly confirmed via analysis of the new metabolite's $^{2-3}J_{H-C}$ HMBC data (Table 1). Inspection of the 2D ^{1}H−^{1}H ROESY spectrum for **10** revealed a correlation between the H-24 methyl protons and the H-26 methyl ester, which suggested an *R* configuration for C-16. In light of the these data and considering that compounds **9** and **10** have a shared biogenic origin, we propose that the absolute configuration of **10** is 3*R*,5*R*,8*S*,9*R*,10*S*,13*R*,14*R*,16*R*.

A substantial portion of the atlantinones' structures are similar to other fungal-derived meroterpenoids such as citreohybriddiones A and B.[34] This group of compounds is proposed to arise from the *C*-alkylation of 3,5-dimethylorsellinate with farnesyl diphosphate, which is subjected to cyclization and further functionalization, yielding a diverse assemblage of products.[35] Geris and Simpson[35] recently hypothesized that the biosynthetic machinery responsible for generating a wide range of homologous meroterpenoids from *Aspergillus* and *Penicillium* (e.g., andrastins, austins, berkeleyones, penisimplicin, and territonin) is likely achieved by means of structural elaboration upon a shared scaffold. We propose that the atlantinones, which incorporate a unique 6,6-dimethyl-2-oxabicyclo[2.2.2]octan-3-one bridged-bicyclic-ring system, constitute a new branch of unusual structural diversification within this metabolite family.

The preponderance of secondary metabolites in the guttate of epigenetically modified *P. citreonigrum* (Figure 1, C and D) suggests that fungal exudates warrant further exploration as a resource for natural product exploration. Considering the proposed role that guttates might play as nutrient sources for symbiotic microbial species, we rationalized that fungal hosts could incorporate bioactive compounds into exudates to influence the composition of the developing microbial community's structure. Accordingly, we tested **1**−**7**, **9**, and **10** against a panel of bacteria and fungi to ascertain if these compounds exhibited antimicrobial activities. Out of the nine compounds, only **1** and **6** exhibited modest zones of inhibition in a disk diffusion assay at a concentration of 30 μg/6 mm paper disk. Both **1** and **6** inhibited *Staphylococcus epidermidis* (both produced 8 mm zones of inhibition), whereas only **6** inhibited *Candida albicans*, *Candida parapsilosis*, *Candida tropicalis*, and *Candida krusei* (8, 7, 8, and 8 mm zones of inhibition, respectively). In contrast, gentamicin (15 μg/6 mm paper disk) exhibited more substantial zones of inhibition that averaged 8−16 mm against a range of bacteria, while ketoconazole (15 μg/6 mm paper disk) produced zones of inhibition that averaged 15−26 mm against a panel of yeast. The modest antimicrobial activities of the azaphilones were not surprising given the similar results that have been reported for other members of this secondary metabolite family.[36−38] However, we did find that our data stood in disagreement with results that had been recently reported for **7**. Whereas Lucas and colleagues observed modest activity for **7** against *Streptococcus pyogenese*, *Staphylococcus aureus*, *Salmonella typhimurium*, *Escherichia coli*, and *Candida albicans* (13−16 mm zones of inhibition using 100 μg/disk),[29] we observed no activity for this metabolite against 10 Gram-negative and Gram-positive bacteria and five fungi at concentrations ranging up to 135 μg/disk. Further studies of the secondary metabolites found in fungal guttates are required to critically assess their drug discovery potential and to understand their biological functions.

Experimental Section

General Methods. The melting points were obtained on a Mel-Temp capillary melting point apparatus. Optical rotations were measured on a Rudolph Research Autopol III automatic polarimeter. The UV and IR data were collected on Hewlett-Packard 8452A diode array and Biorad FTIR FTS 135 spectrometers, respectively. NMR data were obtained on Varian VNMR spectrometers (400 and 500 MHz for ^{1}H, 100 and 125 MHz for ^{13}C) with broad band and triple resonance probes at 20 ± 0.5 °C. Electrospray-ionization mass spectrometry data were obtained on a LCT Premier (Waters Corp.) time-of-flight instrument. HPLC separations were performed on a Shimadzu system using a SCL-10A VP system controller and Gemini 5 μm C_{18} column, (110 Å, 250 × 21.2 mm) with flow rates of 1 to 10 mL/min. X-ray diffraction data were collected on a Bruker-AXS with an APEX CCD area detector with a Cu X-ray source. All solvents were of ACS grade or better.

Organism Collection, Identification, and Culture Methods. A soil sample (~100 g taken from about 20 cm below the soil surface) was collected in a small patch of remnant forest near the coast of Joao Pessoa, State of Paraíba, Brazil, in January 2006. Samples (1 g) were placed in autoclaved H_2O (10 mL) and diluted 10- and 100-fold. Aliquots (300 μL) of the diluted soil suspensions were lawned onto the surfaces of 10 cm diameter Petri plates containing potato-dextrose agar with chloramphenicol (100 mg/L) and cycloheximide (100 mg/L). Plates were maintained at 20 °C for four weeks, and emerging colonies were picked from the plates and transferred to fresh Petri plates containing potato-dextrose agar with chloramphenicol (100 mg/L). This process was repeated for each isolate until a uniform fungal colony was established. Fungi were transferred to new Petri plates containing potato-dextrose agar, and after 2−3 weeks of incubation at 20 °C, pieces of the agar containing mycelia (~0.5 cm^2) were cut and placed in cryogenic storage tubes with sterile glycerol−H_2O (15:85). The tubes were then stored at −80 °C until the fungus was needed for scale-up studies. The fungus was identified by comparative sequence analysis of a 321-base-pair portion of its large ribosomal subunit 28S rRNA gene to data publically available through the NCBI database using a previously published method.[4] A BLAST comparison of our data to the NCBI collection revealed that our fungus was identical to the sequence of a *Penicillium citreonigrum* (syn. *Eupenicillium hirayamae* AF033418; NCBI taxonomic ID: 91632). Frozen samples of this specimen are maintained in the University of Oklahoma Natural Products Discovery Group Collection (sample B004).

For the preparative-scale grow-up, fungal mycelia and spores were inoculated into 50 mL of potato-dextrose media and grown for one week with shaking (125 rpm). The cellular material was placed in a sterile Falcon tube and mixed by vortexing for several minutes to create a uniform fungal cell/spore suspension. Aliquots (500 μL) of the fungal suspension were used to inoculate 110 Erlenmeyer flasks (1 L) containing autoclaved media (0.1 g rice, 0.1 g oatmeal, 0.1 g cornmeal, 0.32 g nutrient broth, ~0.5 g vermiculite, and 50 mL deionized H_2O). Epigenetically modified cultures were treated with 50 μM 5-azacytidine, while the control cultures were treated with vehicle only (filter-sterilized H_2O). Culture vessels were maintained on the benchtop at 25 °C for 20 days.

Extraction and Isolation. The guttate-covered mycelia mats were washed by adding 100 mL of EtOAc to each flask and gently swirling the contents. The liquid was decanted from the flasks, pooled, and placed in a separatory funnel. The organic layer was recovered, and the solvent was removed under vacuum. The resulting organic extract was resolubilized in MeOH and partitioned three times against an equal volume of hexane. Solvent from the defatted MeOH extract was removed under vacuum, which yielded a rust-colored extract (0.8 g). The extract was subjected to gradient C_{18} HPLC (mobile phase 20% to 100% MeOH in H_2O), which yielded three fractions containing secondary metabolites: fraction A (40 mg of **7**), fraction B (160 mg mixture containing **9** and **10**), and fraction C (182 mg mixture containing azaphilones **1**−**6**). Fraction B was subjected to repeated semipreparative C_{18} HPLC (mobile phase 75% to 100% MeOH in H_2O), which provided **9** (7 mg) and **10** (3 mg). The azaphilones in fraction C were purified in two additional steps. The first step consisted of passing the mixture over silica gel in a step gradient fashion with hexane and increasing amounts (10% increments) of acetone. The second step involved applying a portion of the fractions containing the azaphilones to semipreparative C_{18} HPLC (mobile phase 80% to 100% MeOH in H_2O) to give purified **1** (2 mg), **2** (1 mg), **3** (1 mg), **4** (1 mg), **5** (1 mg), and **6** (27 mg).

Sclerotioramine (6): red solid; ^{1}H NMR (400 MHz, $CDCl_3$) δ_H 7.80 (1H, s, H-1), 6.79 (1H, s, H-4), 6.10 (1H, d, J = 16.0 Hz, H-9), 6.95 (1H, d, J = 16.0 Hz, H-10), 5.68 (1H, d, J = 9.8 Hz, H-12), 2.47 (1H, m, H-13), 1.44 (1H, m, H-14), 1.34 (1H, m, H-14), 0.88 (3H, t, J = 7.4 Hz, H-15), 1.04 (3H, d, J = 6.7 Hz, H-16), 1.85 (3H, s, H-17), 1.58 (3H, s, H-18), 2.23 (3H, s, H-20); ^{13}C NMR (100 MHz, $CDCl_3$) δ_C 138.4 (CH, C-1), 146.1 (C, C-3), 110.5 (CH, C-4), 146.6 (C, C-4a), 102.1 (C, C-5), 183.1 (C, C-6), 85.6 (C, C-7), 193.4 (C, C-8), 114.2 (C, C-8a), 116.3 (CH, C-9), 143.0 (CH, C-10), 132.1 (C, C-11), 149.1 (CH, C-12), 35.3 (CH, C-13), 30.2 (CH_2, 14), 12.2 (CH_3, C-15), 20.3 (CH_3, C-16), 12.6 (CH_3, C-17), 23.7 (CH_3, C-18), 171.4 (C, C-19), 20.8 (CH_3, C-20); HRESIMS m/z [M + Na]$^+$ 412.1290 (calcd for $C_{21}H_{24}ClNO_4Na$, 412.1292).

Pencolide (7): white solid; ^{1}H NMR (500 MHz, $CDCl_3$) δ_H 7.40 (1H, q, J = 7.0 Hz, H-3), 1.81 (3H, d, J = 7.0 Hz, H-4), 6.46 (1H, q, J = 2.0 Hz, H-4′), 2.13 (3H, d, J = 2.0 Hz, H-6′); ^{13}C NMR (125 MHz, $CDCl_3$) δ_C 167.3 (C, C-1), 123.0 (C, C-2), 145.3 (CH, C-3), 14.7 (CH_3, C-4), 170.2 (C, C-2′), 146.7 (C, C-3′), 128.3 (CH, C-4′), 169.1 (C, C-5′), 11.7 (CH_3, C-6′); HRESIMS m/z [M + Na]$^+$ 218.0432 (calcd for $C_9H_9NO_4Na$, 218.0429).

Atlantinone A (9): colorless, crystalline solid (MeOH); mp 174−176 °C; $[\alpha]^{21}_D$ −102 (c 0.023, MeOH); UV($CHCl_3$) λ_{max} (log ε) 246 nm (3.83), 298 nm (3.26); FTIR (MeOH) ν_{max} 2946, 2833, 1660,1650, 1029 cm^{-1}; ^{1}H and ^{13}C NMR data, see Table 1; HRESIMS m/z 465.2256 [M + Na]$^+$ (calcd for $C_{26}H_{34}O_6Na$, 465.2253).

Atlantinone B (10): colorless, crystalline solid; [α] (sample degraded before specific rotation data were obtained); ^{1}H and ^{13}C NMR data, see Table 1; HRESIMS m/z 481.2203 [M + Na]$^+$ (calcd for $C_{26}H_{34}O_7Na$, 481.2202).

Preparation of Pencolide Methyl Ester (8). Thionyl chloride (12 mg, 0.10 mmol) was slowly added to a solution of dry MeOH (1 mL) and pencolide (**7**, 11 mg, 0.051 mmol) under a N_2 atmosphere at 0 °C. The mixture was allowed to slowly warm to room temperature with stirring. After 12 h, the excess MeOH was removed under high vacuum and the crude material was subjected to partitioning with EtOAc and H_2O. The organic layer was collected, dried by passing over magnesium

sulfate, and filtered, and the solvent was removed under vacuum. The sample was then subjected to HPLC (C_{18}, 5% to 15% MeOH in H_2O), providing pencolide methyl ester (**8**) in 59% yield (6 mg, 0.030 mmol): ^{1}H NMR (400 MHz, $CDCl_3$) δ_H 7.30 (1H, q, J = 7.2 Hz, H-3), 1.77 (3H, d, J = 7.2 Hz, H-4), 6.44 (1H, q, J = 2.0 Hz, H-4′), 2.13 (3H, d, J = 2.0 Hz, H-6′), 3.73 (3H, s, $COOCH_3$); ^{13}C NMR (100 MHz, $CDCl_3$) δ_C 163.3 (C-1), 123.3 (C-2), 143.5 (C-3), 14.5 (C-4), 170.3 (C-2′), 146.7 (C-3′), 128.3 (C-4′), 170.3 (C-5′), 11.5 (C-6′), 52.8 ($COO\underline{C}H3$).

X-ray Crystallographic Analysis of Atlantinone A (9). $C_{26}H_{34}O_6 \cdot CH_4O$, fw = 474.57, orthorhombic, $P2_12_12_1$, a = 12.0199(6) Å, b = 13.7713(6) Å, c = 14.8276(8) Å, volume = 2454.4(2) Å^3, Z = 4, ρ_{calc} = 1.284 Mg/m^3, Cu Kα radiation, λ = 1.54178 Å. Intensity data were collected on a Bruker instrument with an APEX detector and a graphite-monochromated sealed tube source at a temperature of 100 K. A total of 26 979 data points were collected using ω and ϕ oscillation frames to give 4555 unique data points out to 67° θ with a R_{int} = 0.0476 and 100% coverage. All data were included in the refinement of F^2 values. Hydrogens bonded to carbons were included with assumed geometries and refined with a riding model. Hydrogens bonded to oxygens were located on a difference map, and their positions were refined independently. Final wR2 = 0.0802, R1 = 0.327, S = 1.001.

Analysis of Guttate Metabolites. Cultures treated with 50 μM 5-azacytidine and vehicle controls were prepared in triplicate using the method described for the scale-up metabolite isolation studies (*vide supra*). The cultures were incubated for 20 days, and the guttates were sampled by pinching them off at their bases from the mycelia surface using a pair of fine-tip forceps. We initially experimented with employing a syringe to aspirate the guttate, but were not able to use this approach in light of the fact that both the control and treatment group guttates were quite resinous in consistency. Instead, a total of 25 equal-sized guttate droplets were freed from the mycelia in control and treated cultures and were placed in separate Eppendorf tubes. Control and treated guttates were washed three times with 500 μL of MeOH, and the organic extracts were centrifuged to remove solids. The MeOH-soluble materials were passed over a C_{18} SPE cartridge and subjected to C_{18} HPLC (mobile phase 30% to 100% acetonitrile in H_2O) with parallel ESIMS analysis. Standards consisting of purified **1**−**7**, **9**, and **10** were used to authenticate components in the treated and control samples.

Antimicrobial Assay. Compounds were tested for antimicrobial activity using a disk-diffusion assay. Seed cultures of eight bacteria (*Staphylococcus aureus* ATCC 700787, *Staphylococcus epidermidis* ATCC 12228, *Burkholderia cepacia* ATCC 25608, *Klebsiella pneumoniae* ATCC 33495, *Actinobacter baumannii* ATCC 19606, *Pseudomonas aeruginosa* ATCC 10145, *Escherichia coli* ATCC 11775, and *Enterobacter cloacae* ATCC 13047) and five fungi (*Candida albicans* ATCC 12983, *Candida parapsilosis* ATCC 12969, *Candida glabrata* NRRL Y-65, *Candida tropicalis* ATCC 12968, and *Candida krusei* ATCC 27803) were prepared by incubating the organisms for 10 h at 30 °C (fungi) or 37 °C (bacteria). Aliquots of the overnight cultures (80 μL) were lawned onto the surfaces of nutrient agar (bacteria) or yeast extract agar with 2% (w/v) glucose (fungi). Sterile filter disks (6 mm diameter) infused with 3 μL of test solution (10 μg/μL DMSO), positive control (5 μg/μL DMSO gentamicin for bacteria or 5 μg/μL DMSO ketoconazole for fungi), or vehicle only (DMSO) were added to the plates. The plates were left upright for 30 min at room temperature before being placed in an incubator at 30 °C (fungi) or 37 °C (bacteria). After 10 h, the diameters of the zones of growth inhibition around each disk were recorded.

Acknowledgment. Financial support for this project was provided in part through a grant from the National Institutes of Health (5R01AI085161-02) and funds from the University of Oklahoma College of Arts and Sciences and the Department of Chemistry and Biochemistry. The X-ray diffractometer was purchased through a grant from the NSF (CHE-0130835), and the 400 MHz NMR spectrometer was obtained through a NSF CRIF MU grant (CHE-0639199). A scholarship from CAPES/CNPq-Brazil and assistance rendered by J. M. Barbosa Filho to J.G.S.F. are appreciated.

Supporting Information Available: NMR (^{1}H and ^{13}C NMR, HSQC, HMBC, COSY, and ROESY) data for compounds **6**, **7**, **9**, and **10** and ^{1}H NMR and 1D difference NOE data for **8** are provided. This information is available free of charge via the Internet at http://pubs.acs.org.

References and Notes

(1) Cichewicz, R. H. *Nat. Prod. Rep.* **2010**, *27*, 11–22.
(2) Fisch, K. M.; Gillaspy, A. F.; Gipson, M.; Henrikson, J. C.; Hoover, A. R.; Jackson, L.; Najar, F. Z.; Waegele, H.; Cichewicz, R. H. *J. Ind. Microbiol. Biotechnol.* **2009**, *36*, 1199–1213.
(3) Henrikson, J. C.; Hoover, A. R.; Joyner, P. M.; Cichewicz, R. H. *Org. Biomol. Chem.* **2009**, *7*, 435–438.
(4) Williams, R. B.; Henrikson, J. C.; Hoover, A. R.; Lee, A. E.; Cichewicz, R. H. *Org. Biomol. Chem.* **2008**, *6*, 1895–1897.
(5) Morellato, L. P. C.; Haddad, C. F. B. *Biotropica* **2000**, *32*, 786–792.
(6) Carnaval, A. C.; Hickerson, M. J.; Haddad, C. F. B.; Rodrigues, M. T.; Moritz, C. *Science* **2009**, *323*, 785–789.
(7) Hutwimmer, S.; Wang, H.; Strasser, H.; Burgstaller, W. *Mycologia* **2009**, *102*, 1–10.
(8) Colotelo, N.; Sumner, J. L.; Voegelin, W. S. *Can. J. Microbiol.* **1971**, *17*, 1189–1194.
(9) Colotelo, N. *Can. J. Microbiol.* **1973**, *19*, 73–79.
(10) Colotelo, N. *Can. J. Microbiol.* **1978**, *24*, 1173–1181.
(11) Gareis, M.; Gareis, E.-M. *Mycopathologia* **2007**, *163*, 207–214.
(12) Jennings, D. H. *Mycol. Res.* **1991**, *95*, 883–884.
(13) McPhee, W. J.; Colotelo, N. *Can. J. Bot.* **1977**, *55*, 358–365.
(14) Willmann, G.; Fakoussa, R. *Fuel Process. Technol.* **1997**, *52*, 27–41.
(15) Singh, T.; Arora, D. K. *Microbiol. Res.* **2001**, *156*, 343–351.
(16) Sun, Y.-P.; Unestam, T.; Lucas, S. D.; Johanson, K. J.; Kenne, L.; Finlay, R. *Mycorrhiza* **1999**, *9*, 137–144.
(17) de Boer, W.; Folman, L. B.; Summerbell, R. C.; Boddy, L. *FEMS Microbiol. Rev.* **2005**, *29*, 795–811.
(18) Powell, A. D. G.; Robertson, A.; Whalley, W. B. *Chem. Soc. Spec. Publ.* **1956**, *5*, 27.
(19) Whalley, W. B.; Ferguson, G.; Marsh, W. C.; Restivo, R. J. *J. Chem. Soc., Perkin Trans. 1* **1976**, 1366–1369.
(20) Pairet, L.; Wrigley, S. K.; Chetland, I.; Reynolds, E. E.; Hayes, M. A.; Holloway, J.; Ainsworth, A. M.; Katzer, W.; Cheng, X.-M.; Hupe, D. J.; Charlton, P.; Doherty, A. M. *J. Antibiot.* **1995**, *48*, 913–923.
(21) Seto, H.; Tanabe, M. *Tetrahedron Lett.* **1974**, *15*, 651–654.
(22) Matsuzaki, K.; Tahara, H.; Inokoshi, J.; Tanaka, H.; Masuma, R.; Omura, S. *J. Antibiot.* **1998**, *51*, 1004–1011.
(23) Eade, R. A.; Page, H.; Robertson, A.; Turner, K.; Whalley, W. B. *J. Chem. Soc.* **1957**, 4913–4924.
(24) Wei, W.-G.; Yao, Z.-J. *J. Org. Chem.* **2005**, *70*, 4585–4590.
(25) Arai, N.; Shiomi, K.; Tomoda, H.; Tabata, N.; Yang, D. J.; Masuma, R.; Kawakubo, T.; Omura, S. *J. Antibiot.* **1995**, *48*, 696–702.
(26) Whalley, W. B. *Pure Appl. Chem.* **1963**, *7*, 565–588.
(27) Birkinshaw, J. H.; Kalyanpur, M. G.; Stickings, C. E. *Biochem. J.* **1963**, *86*, 237–243.
(28) Takahashi, J. A.; Castro, M. C. M. d.; Souza, G. G.; Lucas, E. M. F.; Bracarense, A. A. P.; Abreu, L. M.; Marriel, I. E.; Oliveira, M. S.; Floreano, M. B.; Oliveira, T. S. *J. Med. Mycol.* **2008**, *18*, 198–204.
(29) Lucas, E. M. F.; Monteiro de Castro, M. C.; Takahashi, J. A. *Braz. J. Microbiol.* **2007**, *38*, 785–789.
(30) Sutherland, J. K. *Biochem. J.* **1963**, *86*, 243.
(31) Strunz, G. M.; Ren, W.-Y. *Can. J. Chem.* **1976**, *54*, 2862–2864.
(32) Srinivasan, A.; Richards, K. D.; Olsen, R. K. *Tetrahedron Lett.* **1976**, *17*, 891–894.
(33) Shiomi, K.; Uchida, R.; Inokoshi, J.; Tanaka, H.; Iwai, Y.; Omura, S. *Tetrahedron Lett.* **1996**, *37*, 1265–1268.
(34) Kosemura, S. *Tetrahedron* **2003**, *59*, 5055–5072.
(35) Geris, R.; Simpson, T. J. *Nat. Prod. Rep.* **2009**, *26*, 1063–1094.
(36) Quang, D. N.; Hashimoto, T.; Stadler, M.; Radulovic, N.; Asakawa, Y. *Planta Med.* **2005**, *71*, 1058–1062.
(37) Quang, D. N.; Hashimoto, T.; Fournier, J.; Stadler, M.; Radulovic, N.; Asakawa, Y. *Tetrahedron* **2005**, *61*, 1743–1748.
(38) Stadler, M.; Quang, D. N.; Tomita, A.; Hashimoto, T.; Asakawa, Y. *Mycolog. Res.* **2006**, *110*, 811–820.

NP100142H